

Construction of personalized computational phantoms of pregnant patients for assessment of CT radiation dose

Tianwu Xie¹, Pierre-Alexandre Poletti¹, Christoph Becker¹ and Habib Zaidi^{1,2*}

¹Department of Medical Imaging and Information Sciences, Geneva University Hospital, CH-1211 Geneva 4, Switzerland

²Department of Nuclear Medicine and Molecular Imaging, University Medical Center Groningen, Groningen, Netherlands

Abstract—The use of x-ray computed tomography (CT) has increased drastically worldwide during the last two decades and is nowadays playing a pivotal role in clinical diagnosis and radiation therapy planning. The radiation dose delivered to the fetus during CT imaging procedures of pregnant patients raised health concerns because of the high radiosensitivity of the developing embryo/fetus. To assess the diagnostic benefits considering the radiation risks, the radiologist needs reasonably accurate and detailed estimates of the fetal dose from diagnostic CT imaging protocols. To produce realistic biological and physical representations of pregnant patients and embedded fetus, we developed a methodology for construction of patient-specific voxel-based computational phantoms based on existing standardized hybrid computational pregnant female phantoms. We estimated the maternal absorbed dose and fetal organ dose for pregnant patients referred to the emergency unit of Geneva University Hospital for abdominal CT scans. The N-Particle eXtended (MCNPX) general purpose Monte Carlo code was used for radiation transport simulation. The obtained results were compared to those reported by Radimetrics™ (Bayer Healthcare) dose tracking software. The estimated effective dose to the mother varied from 1.1 mSv to 2.0 mSv with an average of 1.6 mSv while Radimetrics™ commercial dose tracking software reported an average effective dose of 1.9 mSv. The normalized fetal dose is about 9.2 mGy/100mAs. The fetus brain and bone marrow receive an average dose of 3.11 ± 1.09 mGy and 1.44 ± 0.45 mGy, respectively. The methodology developed for construction of personalized computational models can be exploited to estimate patient-specific radiation dose from CT imaging procedures. The generated dosimetric data can be used for accurate assessment of the radiation risks to the pregnant patient and fetus from various CT scanning protocols, thus guiding the decision making process.

Index Terms—Computational phantoms, radiation dosimetry, Monte Carlo, x-ray CT imaging

I. INTRODUCTION

Pregnant females represent a critical subpopulation for which absorbed doses from radiologic imaging procedures must be evaluated to make critical decisions regarding the outcome of the developing fetus. Over the period 1997-2006, the number of CT examinations performed on pregnant patients in the US has increased by over 400%. A similar trend is also observed in molecular and hybrid imaging technologies. This increase has led to increasing health concerns regarding the radiation risks to the fetus. At fetal doses greater than 50 mGy, the potential hazard effects of radiation on the fetus include embryonic death, intra-uterine growth limitation, average intelligence quotient (IQ) loss, mental retardation, organ malformation, small head size. Stochastic effects such as cancer and organ-specific

disease might also occur at fetal doses below 50 mGy. The fetal nervous system exhibits a longer period of sensitivity to ionizing radiation than other fetal tissues and is also known to be affected by radiation exposure above 5 mGy. The increased absolute incidence for childhood cancer is 0.017% per mGy while the excess relative risk for leukemia and brain tumors are 0.036 and 0.023 per mGy, respectively.

Accurate estimation of fetal absorbed dose from CT examinations is an immense challenge to the radiologist owing to the difficulties of direct measurement of energy deposition in the fetal body during CT examinations. Techniques based on experimental measurement of physical phantoms or simulations using simplified phantoms have been adopted for estimating fetal absorbed dose, including Monte Carlo simulations using computational anthropomorphic models [1-7] and measurements using physical phantoms with embedded dosimeters [8-12]. However, the accuracy of these estimates is limited by assumptions inherent to the measurement/simulation setup and significant overestimation or underestimation of the fetal absorbed dose might occur [13]. While on-the-fly Monte Carlo calculations are considered as reference (gold standard) for dose estimation in diagnostic imaging [14-18], implementation of a framework for patient-specific estimation of fetal dose in clinical setting is highly desired.

In this work, we propose a methodology for the construction of patient-specific computational models based on image segmentation and registration methods and previously developed standardized hybrid computational phantoms[19]. Monte Carlo simulations were used for the calculation of fetal/maternal organ/tissue absorbed doses and compared with the results provided by the Radimetrics™ commercial dose tracking software [20].

II. METHODS

A. Construction of patient-specific computational models

A series of ICRP-based pregnant female computational phantoms were developed and were used as anchor models for the construction of patient-specific models. CT images of seven patients were segmented and utilized for the construction of regional voxel-based models. The developed anchor models were registered to regional patient-specific voxel-based models using a 3-D deformable registration algorithm to produce new personalized pregnant phantoms with well-defined anatomical structures, matching patient images obtained from CT examinations. Image registration was performed using the

Insight Toolkit (ITK, <https://itk.org/ItkSoftwareGuide>) [21]. The personalized voxel-based pregnant phantoms were used as input for MCNPX-based Monte Carlo calculations of CT radiation dose to the fetus and maternal body. Each patient-specific computational model includes 35 identified maternal organs (adrenals, brain, breasts, esophagus, eyeballs, eye lens, gallbladder wall, gallbladder content, heart wall, heart content, kidney, large intestine wall, large intestine content, liver, lungs, ovaries, pancreas, small intestine, skeleton, skin, spleen, stomach wall, stomach content, thymus, thyroid, trachea, remainders, urinary bladder wall, urinary bladder content, uterine wall, uterine content, placenta, umbilical cord, amniotic fluid and vesicle vitelline) and 25 fetal organs (soft tissue, skeleton, bone marrow, brain, esophagus, eyes, thyroid, spinal cord, lungs, heart, kidneys, liver, stomach, gall bladder, salivary gland, large intestine, small intestine, urinary bladder, skin, ovaries, testis, adrenal, pancreas, spleen and thymus). The uterus of the developed patient-specific computational phantoms including the embedded fetus and other tissues, were adjusted through registration to the segmented uterus region from patients' CT images.

TABLE I. COMPARISON BETWEEN MONTE CARLO SIMULATED AND MEASURED CT RADIATION DOSE IN AIR, HEAD AND BODY PHANTOMS.

120 kVp tube voltage	Head	Body
Absorbed dose per photon (mGy)	1.88E-14	6.64E-15
Number of photons (1/Angle.mAs)	1.52E+12	1.26E+12
Simulated dose (mGy/100mAs)	19.9	5.8
Measured dose (mGy/100mAs)	19.9	6
Percent difference (%)	0.03%	-3.5%

B. CT dose calculations

A VCT 750HD (General Healthcare) CT scanner installed in the emergency unit of Geneva University Hospital was used in all measurements and Monte Carlo simulations. This CT scanner was equipped with Performix Pro VCT 100 x-ray tube with 56 degree fan-beam angle, 7 degree target angle and allowing for selection of a beam collimation thickness of 1.25 - 40 mm. The quality equivalent filtration of the x-ray tube is calculated at a nominal thickness value of 4.3 mm of aluminum. The source to isocentre distance on this CT scanner is 54 cm, while the source to detector distance is 95 cm. The geometry modeling of the CT gantry was performed and validated in previous works. The MCNPX code was used for Monte Carlo simulations of the x-ray source and CT gantry. The x-ray energy spectrum was generated using SpekCalc for 120 kVp tube voltage. Simulations were conducted mimicking the clinical acquisition protocol, using a table speed (55 mm/rot), scan range and 40 mm collimation.

C. Dose measurements in air and cylindrical phantoms

To quantify the absolute outputs of the x-ray tube for converting Monte Carlo results to measured absorbed dose, free-in-air dose was measured using a calibrated ion chamber with 10 cm effective length and 2.844 cm³ air cavity. The ion chamber was positioned at the isocenter of the CT scanner with its long axis aligned with the axis of gantry rotation. Helical axial scans were performed along the effective length of the ion

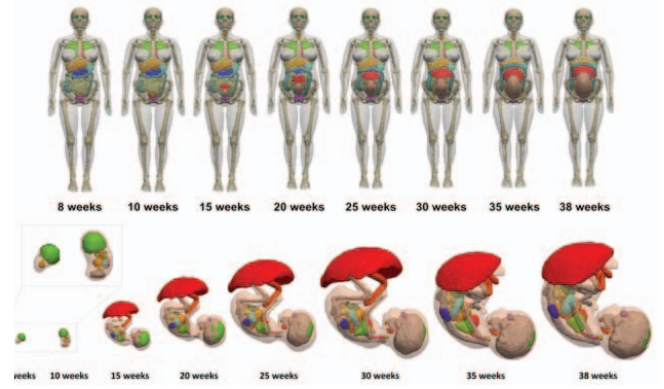


Figure 1. Anchor phantoms of reference pregnant female and fetus at various gestation ages.

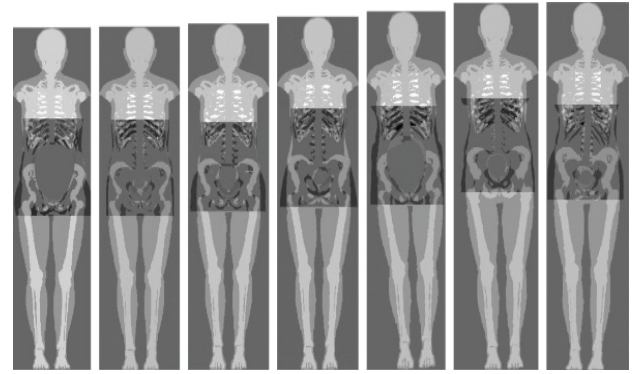


Figure 2. Examples of the generated patient-specific computational models with overlaid patient CT images.

chamber. Two PMMA phantoms representing the head and body with 16 cm and 32 cm diameter were further used for verification of the Monte Carlo code. Radial dose distributions in the phantom from helical axial scans were measured with the ion chamber. The energy deposited in its air cavity was obtained and recorded as $D_{measured,in\ air}$. Monte Carlo simulations were then performed for the detector in air under the same conditions. The simulated free-in-air exposure values of the ion chamber was recorded as $D_{simulated,in\ air}$. The ratio of the measured to the simulated in-air dose refers to the conversion coefficient from simulated results to physical absolute dose and is defined as the output correction factor (OCF) [22]:

$$OCF = \frac{D_{measured,in\ air}}{D_{simulated,in\ air}} \quad (1)$$

In this study, the measured and simulated free-in-air doses at 120 kVp tube voltage were 33.8 mGy/100mAs and 4.8 mGy/100mAs, respectively, with a calculated OCF value of 3.5.

The measurements using cylindrical phantoms were performed by positioning the ion chamber at the center of the cylindrical phantoms to obtain measured absorbed doses of $D_{measured,head}$ and $D_{measured,body}$, respectively, after performing CT examinations along the length of the cylindrical phantoms. To include the scatter tails at the beginning and the end of CT scans of the CTDI phantom, the 5 cm axial field-of-view (FOV) was set along the center of the

10 cm pencil chamber. The absorbed doses in the computerized CT dosimetry phantoms were calculated as:

$$D_{estimated} = d_{simulated} \times n \times \Omega \times mAs \times OCF \quad (2)$$

where $d_{simulated}$ is the absorbed dose per photon emitted from the source obtained in simulations, n is the number of photons emitted from the source per solid beam angle per mAs, calculated from *SpekCalc* [23] simulated x-ray energy spectra, Ω is the solid angle of the fan beam, mAs is the effective tube current-time product value and OCF is the estimated output correction factor.

D. CT acquisitions of clinical studies

The pregnant patients referred to the emergency unit of Geneva University Hospital for abdominal CT scans between march 2011 and september 2015. Low-dose CT examinations were performed using 120 kVp, 1.25 mm slice thickness, a pitch of 1.375:1, 31.5 mAs without tube current modulation. Patient ages varied from 19 years to 45 years while the gestation period ranged between 8 weeks and 35 weeks. CT images were pushed on Radimetrics™ dose tracking software for calculation of maternal and fetal effective dose. The results were further compared with those obtained using the proposed method and Monte Carlo calculations.

E. Absorbed Dose Calculations for Pregnant Patients and Fetus

The energy deposited in organs were recorded using F6 tally in the MC code and used to calculate the absorbed dose from invested CT scans according to Equation (2). To reflect the combined detriment from stochastic effects of equivalent doses in all organs of the human body, the concept of effective dose was introduced [24], and is defined as:

$$ED = \sum_T \omega_T \sum_R \omega_R D_{R,T}, \quad (3)$$

where E is the effective dose, ω_R is the radiation weighting factor for radiation type R , $D_{R,T}$ is the contribution of radiation type R to the absorbed dose, and ω_T is the tissue weighting factor for organ/tissue T reflecting its relative radiation sensitivity.

Subsequently, clinical CT images for each patient were imported into Radimetrics™ dose tracking software [20] for calculation of maternal and fetal effective dose, as shown in Figure 3.

III. RESULTS

A. Computational phantoms

Figure 1 illustrates the anchor phantoms of reference pregnant female and fetus at various gestation ages. Figure 2 shows the generated patient-specific computational models with overlaid abdominal CT images.

B. Validation of the simulation model

Table 1 summarizes the validation for developed Monte Carlo model. The differences between simulated and measured radiation dose range between -3.5% and 0.03%. The output

correction factor is calculated based on the free-in-air measured/simulated doses in the ion chamber.

C. Absorbed dose and effective dose for pregnant patients

The estimated fetal total body dose is about 2.11 ± 0.37 mGy while Radimetrics™ reported 2.47 ± 0.42 mGy. The average absolute differences of estimated fetal and uterus doses between Monte Carlo simulations and Radimetrics™ are about 21% and 31%, respectively.

TABLE II. AVERAGED ABSOLUTE FETAL DOSE FOR DIFFERENT FETAL ORGANS.

Fetal organs	Average absolute fetal dose (mGy)
Adrenal	1.67 ± 0.29
Bone marrow	3.11 ± 1.09
Brain	1.44 ± 0.45
Esophagus	1.37 ± 0.27
Eyes	1.12 ± 0.31
Gall bladder	1.62 ± 0.24
Heart	1.66 ± 0.34
Kidneys	1.87 ± 0.30
LI	1.65 ± 0.27
Liver	1.78 ± 0.31
Lungs	1.70 ± 0.31
Pancreas	1.73 ± 0.30
SI	1.69 ± 0.26
Skeleton	5.98 ± 1.66
Skin	1.70 ± 0.31
Slivary Grand	1.17 ± 0.29
Soft tissue	1.70 ± 0.31
Spinal cord	1.67 ± 0.28
Spleen	1.83 ± 0.28
Stomach	1.72 ± 0.30
Testis	1.50 ± 0.21
Thymus	1.36 ± 0.26
Thyroid	1.51 ± 0.41
UB	1.72 ± 0.29
Total body	2.11 ± 0.37

This study estimated a detailed organ-level radiation doses to the fetus from CT examinations. It can be observed in Table II that the absorbed dose is non-uniformly distributed between fetal organs where the fetal skeleton and bone marrow receive about 3.8 and 2.0 times higher absorbed doses, respectively, than other fetal tissues. The dependence of fetus total body dose upon maternal perimeter given by Angel *et al.* [1] is shown for comparison (the red dash line in Figure 4). There are significant correlations between fetal brain dose and the parameters of conceptus depth, gestational age and maternal size. The absorbed doses to some organs, such as the kidney, gall bladder, urinary bladder, large intestine, small intestine, etc., also present insignificant correlations with considered three considered anatomical parameters.

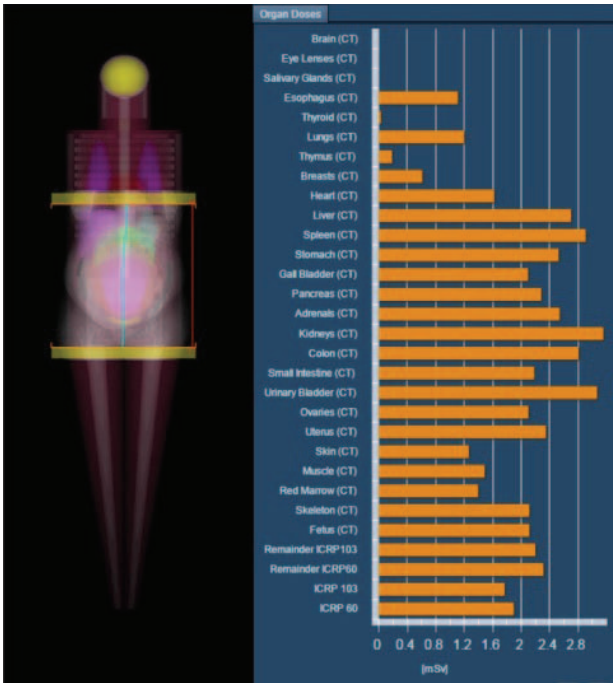


Figure 3. Principle of dose estimation using Radimetrics™ showing the matching of patient CT images with the stylized computational phantom (left) and the estimated organ-level absorbed doses (right).

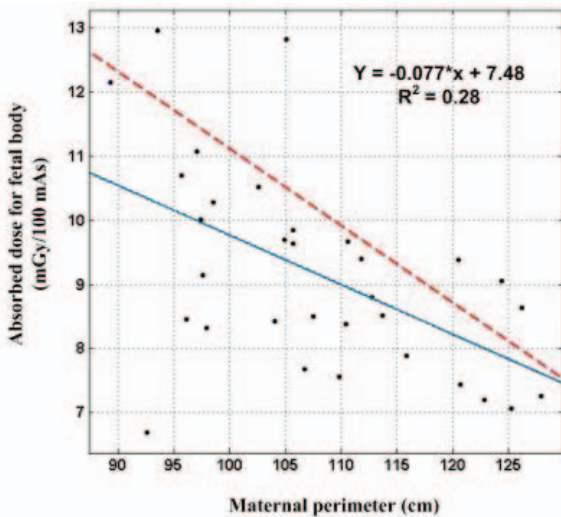


Figure 4. Plots of radiation dose to the fetal body versus. The results for normalized fetus dose vs. maternal perimeter by Angel *et al.*[1] were shown for comparison (red dash line).

IV. CONCLUSION

We implemented a methodological framework for assessment of patient-specific fetal dose. The radiation dose to the fetal body from CT examinations of pregnant patients varies in within the range 6.7-13 mGy/100mAs with a mean value of 9.2 mGy/100mAs while Felmlee *et al.* [25], Angel *et al.* [1] and Damilakis *et al.* [7] reported average fetal doses of 11.3, 10.8 and 22.6 mGy/100 mAs, respectively. The fetal

organ-level radiation dose from CT examinations is rarely reported in literature. However, the fetal skeleton and bone marrow receive significantly higher absorbed dose than other soft tissues. Since radiation exposure of bone marrow and brain in childhood may increase the risk of leukemia and brain tumors [26], the absorbed dose to fetal bone marrow and fetal brain during CT examinations of pregnant patients is an important matter of concern for the radiologist and the patient.

The mean fetal total body dose estimated in this work for the investigated patient cohort is consistent with results reported in the literature but lower than the estimates provided by Radimetrics™ dose tracking system. This discrepancy may be attributed to the utilization of simplistic stylized pregnant female phantoms and other many other approximations and assumptions made by Radimetrics™.

Patient-specific computational models can be created based on the developed standardized computational phantoms of pregnant females to reflect personalized body morphometries, thus enabling to perform patient-specific dosimetry for a variety of radiation exposure situations to provide more accurate dosimetric estimates for radiation dose tracking and radiation risk monitoring.

ACKNOWLEDGMENT

This work was supported by the Swiss National Science Foundation under No. 31003A-149957 and Geneva Cancer League.

REFERENCES

- [1] E. Angel, C. Wellnitz and M. Goodsitt, "Radiation Dose to the Fetus for Pregnant Patients Undergoing Multidetector CT Imaging: Monte Carlo Simulations Estimating Fetal Dose for a Range of Gestational Age and Patient Size 1," *Radiology*, vol. 249, pp. 220-227, 2008.
- [2] E. Helmrot, H. Pettersson, M. Sandborg and J. N. Altén, "Estimation of dose to the unborn child at diagnostic X-ray examinations based on data registered in RIS/PACS," *Eur Radiol*, vol.17, pp. 205-209, 2007.
- [3] J. Damilakis, A. Tzedakis, K. Perisinakis and A. E. Papadakis, "A method of estimating conceptus doses resulting from multidetector CT examinations during all stages of gestation," *Med Phys*, vol. 37, pp. 6411-6420,2010.
- [4] H. T. Winer-Muram, J. M. Boone and H. L. Brown, "Pulmonary Embolism in Pregnant Patients: Fetal Radiation Dose with Helical CT 1," *Radiology*, vol. 224, pp. 487-492, 2002.
- [5] J. Gu, X. G. Xu and P. F. Caracappa, "Fetal doses to pregnant patients from CT with tube current modulation calculated using Monte Carlo simulations and realistic phantoms," *Radiat Prot Dosim*, vol. 19, pp. 1-9, 2012.
- [6] X. Lopez-Rendon, M. Walgraeve and S. Woussen, "Comparing different methods for estimating radiation dose to the conceptus," *Eur Radiol*, vol 16, pp. 1-8, 2016.
- [7] J. Damilakis, K. Perisinakis and A. Tzedakis, "Radiation Dose to the Conceptus from Multidetector CT during Early Gestation: A Method That Allows for Variations in Maternal Body Size and Conceptus Position 1," *Radiology*, vol. 257, pp. 483-489, 2010.
- [8] A. Kellaranta, T. Kaasalainen and R. Seuri, "Fetal radiation dose in computed tomography," *Radiat Prot Dosim*, vol. 165, pp. 226-230, 2015.
- [9] T. A. Jaffe, A. M. Neville and C. Anderson-Evans, "Early first trimester fetal dose estimation method in a multivendor study of 16-and 64-MDCT scanners and low-dose imaging protocols," *AJR Am J Roentgenol*, vol. 193, pp. 1019-1024, 2009.
- [10] T. A. Jaffe, T. T. Yoshizumi and G. I. Toncheva, "Early first-trimester fetal radiation dose estimation in 16-MDCT without and with automated

tube current modulation," *AJR Am J Roentgenol*, vol. 190, pp. 860-864, 2008.

- [11] L. C. Chatterson, D. A. Leswick and D. A. Fladeland, "Fetal shielding combined with state of the art CT dose reduction strategies during maternal chest CT," *Eur J Radiol*, vol. 83, pp. 1199-1204, 2014.
- [12] G. Solomou, A. Papadakis and J. Damilakis, "Abdominal CT during pregnancy: a phantom study on the effect of patient centring on conceptus radiation dose and image quality," *Eur Radiol*, vol. 25, pp. 911-921, 2015.
- [13] H. Zaidi and X. G. Xu, "Computational anthropomorphic models of the human anatomy: The path to realistic Monte Carlo modeling in medical imaging," *Annu Rev Biomed Eng*, vol. 9, pp. 471-500, 2007.
- [14] T. Xie and H. Zaidi, "Fetal and maternal absorbed dose estimates for positron-emitting molecular imaging probes," *J Nucl Med*, vol. 55, pp. 1459-1466, 2014.
- [15] T. Xie, W. E. Bolch and C. Lee, "Pediatric radiation dosimetry for positron-emitting radionuclides using anthropomorphic phantoms," *Med Phys*, vol. 40, pp. 102502, 2013.
- [16] T. Xie and H. Zaidi, "Effect of respiratory motion on internal radiation dosimetry," *Med Phys*, vol. 41, pp. 112506, 2014.
- [17] T. Xie and H. Zaidi, "Evaluation of radiation dose to anthropomorphic paediatric models from positron-emitting labelled tracers," *Phys Med Biol*, vol. 59, pp. 1165-1187, 2014.
- [18] H. Zaidi and M. Ay, "Current status and new horizons in Monte Carlo simulation of X-ray CT scanners," *Med Biol Eng Comput*, vol. 45, pp. 809-817, 2007.
- [19] T. Xie and H. Zaidi, "Development of computational pregnant female and fetus models and assessment of radiation dose from positron-emitting tracers," *Eur J Nucl Med Mol Imaging*, vol. 43, pp. 2290-2300, 2016.
- [20] Radimetrics Enterprise Platform: Dose Management Solution, *Bayer HealthCare*, <http://www.radiologysolutions.bayer.com/products/ct/dosemanagement/rep/>, Accessed 2016.
- [21] L. Ibanez, W. Schroeder and L. Ng, "The ITK software guide," 2005.
- [22] X. Li, E. Samei and W. P. Segars, "Patient-specific radiation dose and cancer risk estimation in CT: Part I. Development and validation of a Monte Carlo program," *Med Phys*, vol. 38, pp. 397-407, 2011.
- [23] G. Poludniowski, G. Landry and F. DeBlois, "SpekCalc: a program to calculate photon spectra from tungsten anode x-ray tubes," *Phys Med Biol*, vol. 54, pp. N433, 2009.
- [24] ICRP, "ICRP Publication 103: The 2007 Recommendations of the International Commission on Radiological Protection," *Ann ICRP*, vol. 37, pp. 1-332, 2007.
- [25] J. P. Felmlee, J. Gray and M. Leetzow, "Estimated fetal radiation dose from multislice CT studies," *AJR. AJR Am J Roentgenol*, vol. 154, pp. 185-190, 1990.
- [26] M. S. Pearce, J. A. Salotti and M. P. Little, "Radiation exposure from CT scans in childhood and subsequent risk of leukaemia and brain tumours: a retrospective cohort study," *The Lancet*, vol. 380, pp. 499-505, 2012.